

The Hamiltonian of the V_{15} Spin System from first-principles Density-Functional Calculations

Jens Kortus[†], C. Stephen Hellberg and Mark R. Pederson

Center for Computational Materials Science, Code 6390, Naval Research Laboratory, Washington, DC 20375

(December 2, 2024)

We report first-principles all-electron density-functional based studies of the electronic structure, magnetic ordering and anisotropy for the V_{15} molecular magnet. From these calculations, we determine a Heisenberg Hamiltonian with four antiferromagnetic and one *ferromagnetic* coupling. We perform direct diagonalization to determine the temperature dependence of the susceptibility. This Hamiltonian reproduces the experimentally observed spin $S=1/2$ ground state and low-lying $S=3/2$ excited state. A small anisotropy term is necessary to account for the temperature independent part of the magnetization curve.

75.50.Xx, 75.30.Gw, 75.45.+j, 75.30.Et

With the continued interest in the fabrication and optimization of miniaturized magnetic devices [1] future design considerations will require an understanding of nanoscale magnetic systems. In order to transition such materials into simple devices it is necessary to be able to explain how interactions such as spin-spatial coupling and spin-spin exchange effects may couple collectively to create a seemingly single-spin system. Further, it is necessary to determine the temperature range at which such systems will indeed behave collectively. In general the properties of a nanoscale system of coupled spins depend directly on the strength of the exchange-parameters and on the size and sign of the anisotropy energy due to spin-orbit coupling. While these parameters are generally determined by the transition metal atoms, the ligands and other nonmagnetic atoms are responsible for stabilizing the array of spins. Requisite to a complete computational understanding of such spin systems is the ability to account for the strong ligand-metal interactions and to determine whether the behavior of a given spin system is mainly mediated by the anisotropy, by spin-spin coupling or by a combination of the two.

Recently, the Mn_{12} -Acetate and Fe_8 molecules [2] have attracted considerable interest because they behave as high-single-spin systems (total spin $S=10$) at temperature ranges on the order of 20-60K. Due to their large magneto-molecular anisotropy energy these systems retain their moment orientation at reasonably high temperatures and exhibit the phenomena of resonant tunneling of magnetization at well defined magnetic fields [3,4].

The $K_6[V_{15}As_6O_{42}(H_2O)] \cdot 8H_2O$ molecular crystal, first synthesized by Müller and Döring [5,6], represents a transition-metal spin system in the same size regime as the Mn_{12} and Fe_8 molecular crystals. In contrast to Mn_{12} and Fe_8 molecules, the V_{15} molecule is thought to behave as a weakly anisotropic magnet composed of 15 spin $s=1/2$ particles which couple together to form a molecule with a total spin $S=1/2$ ground state. Besides the fundamental interest in understanding quantum effects in these nanomagnets they might be also relevant

for implementations of quantum computers [7]. Calculations on such correlated systems present a challenge to mean-field frameworks such as density-functional theory because it is often not possible to construct a single collinear reference state which preserves the inherent symmetry of the system and has the correct spin quantum numbers.

This work utilizes an efficient coupled multilevel analysis which relies on fitting density-functional energies to mean-field Heisenberg or Ising energies in order to determine the exchange parameters. The approximate exchange parameters gleaned from the first N Ising configurations were used to find the next lowest energy Ising configuration and subsequently to improve the parameterization of the exchange parameters. “Self Consistency” of this approach is determined when the low-energy predicted Ising levels as well as the low-energy spin-excitation spectrum of the Heisenberg Hamiltonian, obtained from exact diagonalization, are unchanged by the addition of data from new Ising configurations. The coupling of the density-functional method to a classical Ising representation allowed us to determine the exchange parameters by considering only 11-12 spin configurations. Further, the resulting ground-state spin configuration within density-functional theory exhibits the correct spin projection of $\frac{1}{2}$ and is significantly different than what our original guess at the density-functional ground state was.

Starting from X-ray data [8] we generated several unit cells and isolated a single $K_6[V_{15}As_6O_{42}(H_2O)]$ unit. In order to optimize the geometry within the quasi- D_3 symmetry of the V_{15} molecule [5], we replaced the statistically oriented water molecule at the center of the molecule by a neon atom and used an $S=3/2$ spin configuration which does not break the crystallographic symmetry. The Ising configuration of this molecule consists of three aligned spin- $\frac{1}{2}$ V atoms in the triangle and equivalent upper and lower hexagons composed of a ring of antiferromagnetically (AF) coupled spin- $\frac{1}{2}$ V atoms.

The geometry of the molecule was then optimized

within the all-electron density-functional methodology using the generalized-gradient approximation (GGA) [9]. The calculations were performed with the Naval Research Laboratory Molecular Orbital Library (NRLMOL) [10]. Calculations on 49 geometrical configurations were performed during the conjugate-gradient relaxation of the molecule. Subsequent calculations show that the geometrical, electronic and magnetic properties of this system are unaffected by the presence or type of inert moiety enclosed within the void. Using this geometry, we performed eleven additional calculations on different spin configurations (See Table I) to determine the five exchange parameters (J 's) of the Heisenberg Hamiltonian

$$H = \sum J_{ij} \mathbf{S}_i \cdot \mathbf{S}_j, \quad (1)$$

as well as the spin configuration of the density-functional ground state [11]. The J 's used in the above Hamiltonian are defined according to Fig. 1. As shown in Table I, we have included high-spin configurations (X, XI, XII), which generally have some symmetry as well as lower-spin non-symmetric configurations. The energy for the high-spin $S = 15/2$ ferromagnetic (FM) state (XII) of 873 meV is predominantly caused by a large AF exchange coupling (J) between the most closely bonded hexagonal V atoms. However, the 113 meV splitting between the $S=9/2$ and $S=15/2$ states (XI and XII) shows that there is a reasonably strong AF coupling, approximately 18 meV on average, between the triangular and hexagonal atoms. All of the data displayed in Table I has been used to determine the exchange parameters from a least square fit to the mean-field solution of the Heisenberg Hamiltonian (1). The fit is very good with errors ranging from 0.1-1.55 meV. The fit leads to exchange parameters of $J = 290.5$ meV, $J' = -22.8$ meV, $J'' = 15.9$ meV, $J_1 = 13.8$ meV and $J_2 = 23.4$ meV, where positive numbers correspond to AF and negative ones to FM interactions. The *ferromagnetic* interaction J' is the most surprising result and deserves further discussion since it is qualitatively different from earlier assumptions based on entirely AF interactions [6,12]. Ferromagnetic coupling is possible without polarizing the oxygens through a 4'th order process similar to super-exchange. In super-exchange, the intermediate state has the lowest d -orbital on the V doubly occupied with up and down electrons [13]. However, electrons can also hop to higher energy d -orbitals on the V's. In this case both parallel and antiparallel spins are allowed without violating the Pauli exclusion principle, but Hund's rule coupling prefers parallel alignment. The super-exchange process (same d -orbital) completely excludes the process with same-spin electrons while the FM process (different d -orbitals) merely favors FM alignment. Thus a FM coupling is obtained if the V-O hopping matrix elements into the higher d -orbital are significantly larger than the matrix elements for the hopping of O electrons into the lowest energy d -orbital. The occurrence of such interactions are possible in a low-symmetry system

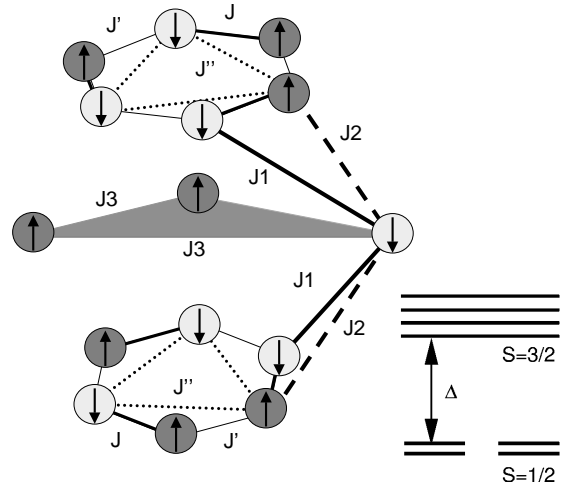


FIG. 1. The 15 magnetic vanadium atoms of the $K_6[V_{15}As_6O_{42}(H_2O)]$ molecule. They form two hexagonal layers and an inner triangular layer of vanadium atoms sandwiched within. The arrows show the lowest energy spin configuration found from DFT calculations. The five exchange parameters used in the Heisenberg Hamiltonian are shown as lines. Schematically displayed are energy levels of the Kramer doublet ($S=1/2$) ground state and the low lying quadruplet ($S=3/2$) separated by Δ .

such as the one studied here.

Even with this FM interaction, our spin Hamiltonian yields an $S=1/2$ ground state composed largely of Ising configurations similar to the one depicted in Fig. 1. This Ising configuration was predicted from the J 's from earlier fits to DFT energies and corresponds to the ground state DFT configuration (I).

TABLE I. DFT energies (E) of calculated Ising configurations, energies obtained from the fit, and $4\langle S_i^z S_j^z \rangle$ along each of the five bonds. Also included is the anisotropy shift δ for the $M_s = S$ state of each Ising configuration. A least square fit of this data leads to exchange parameters of $J=290.5$, $J'=-22.8$, $J''=15.9$, $J_1=13.8$, $J_2=23.4$ meV.

E (meV)	Fit	J	J'	J''	J_1	J_2	Spin	Label	δ (K)
-78.37	-78.27	-6	2	-2	6	-6	1/2	I	0.8
-73.39	-73.47	-6	2	-2	4	-4	1/2	II	
-34.89	-34.75	-6	-2	2	4	-4	3/2	III	
0.00	-0.83	-6	-6	6	6	-6	3/2	IV	1.5
8.38	8.78	-6	-6	6	2	-2	1/2	V	1.3
28.14	27.99	-6	-6	6	-6	6	3/2	VI	
126.32	126.10	-4	-4	6	4	-6	1/2	VII	
129.17	128.79	-4	-4	2	6	-4	5/2	VIII	
278.35	278.54	-2	-6	2	4	-4	3/2	IX	
434.22	435.77	0	0	6	6	0	9/2	X	1.6
760.75	760.76	6	6	6	-6	-6	9/2	XI	1.6
873.11	872.37	6	6	6	6	6	15/2	XII	1.8

We have diagonalized the Heisenberg Hamiltonian (1), finding a spin- $\frac{1}{2}$ Kramer doublet as the ground state

with a low-lying spin- $\frac{3}{2}$ quadruplet as shown in Fig. 1. The rest of the spectrum is well separated from these eight states. The large value of J binds the spins in the hexagons into singlets. The low-energy physics arises from the inner triangle spins interacting with each other with an effective coupling through the hexagons, yielding the doublet-quadruplet spectrum [14]. There are two important energy scales in the spectrum: Δ , the gap between the doublet and quadruplet, and J , the energy at which the singlets in the hexagon break and the molecule starts to behave as more than three spins. The low-energy effective interaction between inner triangle spins proceeds via J_1 and J_2 (which frustrate each other) to a hexagon singlet, via J' and J'' to a neighboring singlet, and finally via J_1 and J_2 . Thus simple perturbation theory [6] yields

$$\Delta = (3/4)(J_2 - J_1)^2(J'' - J')/J^2. \quad (2)$$

Comparing our calculated susceptibility with experiment [12], we find the low-temperature behavior indicates our doublet-quadruplet gap $\Delta \approx 0.4\text{K}$ to be significantly smaller than the experimental value of $\Delta \approx 3.7\text{K}$, while the high-temperature behavior shows our calculated value of J is too large. Both of these discrepancies can be explained almost entirely by a J that is too large within the density-functional-based treatment. We note that all the V-V bond lengths obtained from our DFT optimized geometry (GGA) are too short compared with experiment [15] and both theory and experiment show that the bond distance between the J singlet dimers is the shortest V-V distance. The large value of J can be attributed to both exchange processes through the oxygens and to direct exchange between the V. The potential for direct V-V hopping has been originally raised by Pickett in CaV_4O_9 [16] and similar behavior has been observed in MgVO_3 [17]. All these V compounds are structurally very similar to our V_{15} cluster with the V atom inside a square pyramid of five oxygens. The shortest V-V distance, which is directly related to the value of J , is slightly smaller in our V_{15} cluster than in the case of the mentioned V compounds. If direct exchange is important, the value of J will be influenced greatly by the overlap between the V atoms. In order to determine if our enhanced J may be due to spurious on-site repulsions associated with the DFT, we have approximately accounted for the effects of self-interaction-corrections (SIC) in model calculations on V dimers (V_2 and V_2O_{10}) with electronic structure constrained to match that of the dimers in the V_{15} cluster. The results, while preliminary, show that SIC induced changes in the wavefunctions could decrease the direct contributions to J by a factor of 3 which supports the reduction of J to yield better agreement between experiment and theory.

Reducing J to 70 meV and slightly reducing the difference between J_1 and J_2 yields the effective moment shown in Fig. 2, which agrees very well with experiment. A set of AF interactions [6] also fits the experimental

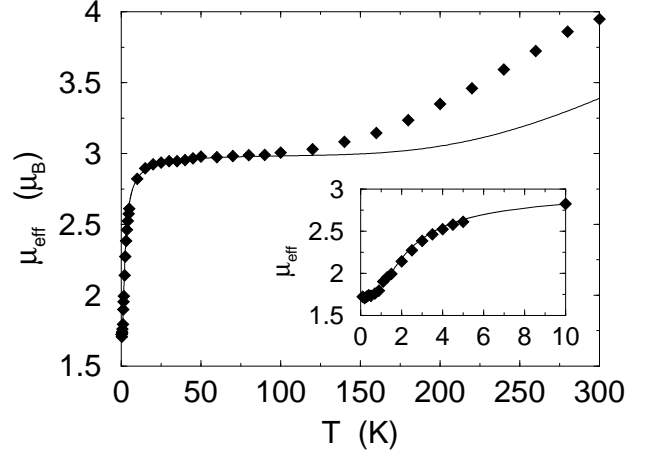


FIG. 2. The effective moment $\mu_{\text{eff}} = \sqrt{3\chi T}$ calculated with $J = 70$ meV and J_1 (J_2) increased (decreased) by 2 meV. All other exchange parameters are unchanged. The inset shows the low temperature behavior.

results. In fact any set of parameters with the correct values of J and Δ given by Eq. (2) will fit the effective moment well. To support future efforts aimed at experimentally confirming our FM J' parameter, we have calculated the spin-spin correlation function $C_S = 4\langle S_i^q \cdot S_j^q \rangle$, with q representing the arbitrary quantization axis. Since J is always largest, the spins tend to form a singlet along this bond, yielding $C_S(J) \cong -1$ (AF correlation). With a reasonable $J = 70\text{meV}$, our FM J' relieves frustration, making the two correlations $C_S(J') \cong +0.11$ and $C_S(J'') \cong -0.12$ about twice as large as they are in the case of AF interactions only [6]. These correlations are FM and AF, respectively, and are robust with respect to small changes in any of the exchange parameters. This prediction should be measurable with neutron scattering.

Chiorescu *et al.* observe that rotation of the spin projection is achieved without encountering a barrier [12] and Dobrovitski *et al.* posit that the V_{15} molecule is indeed a low anisotropy system [14]. Here, we point out that the small splitting between the doublet and quadruplet is an order of magnitude smaller than the anisotropy barriers in the Mn_{12} and Fe_8 systems. Further, if the V_{15} were to possess easy-axis anisotropy with a second-order anisotropy parameter similar to that of Mn_{12} , the effect would be to split the quadruplet into two doublets with the ($M_s=3/2$ and $-3/2$) doublet shifted downwards by 1.25K. This could potentially change the total spin of ground state. As shown below the existence of either easy-plane or easy-axis anisotropy will shift the $M_s=3/2-1/2$ Zener-Landau tunneling transitions that have been observed by Chiorescu *et al.* [12].

Recently, Pederson and Khanna have developed a new method for accounting for second-order anisotropy energies [18]. This method relies on a simple albeit exact method for spin-orbit coupling and a second-order per-

turbative treatment of the spin-orbit operator to determine the dependence of the total energy on spin projection. Initial applications to Mn_{12} lead to a density-functional-based second-order anisotropy energy of 55.7K [19] which is in essential agreement with the experimentally deduced values of 55.6K [20]. We have generalized this methodology to systems with arbitrary symmetry and have calculated the anisotropy energy for several different spin configurations of the V_{15} molecule.

We have calculated the anisotropy energy for the lowest Ising configurations with one, three, nine and fifteen unpaired electrons, as given in Table I. In all cases we find that the V_{15} possesses weak easy-plane anisotropy. This result ensures that anisotropy effects will not change the total spin of the V_{15} ground state. Examination of the expression for the second order anisotropy energy in Ref. [18], shows that such energies do not necessarily scale as the square of the total moment. Indeed, as shown in Table I, we find that the anisotropic effects are in fact only weakly dependent on the total spin and that the energy of the $M_s=S$ state increases by approximately $\delta=0.8\text{K}$ to 1.8K . Chiorescu *et al.* show that the broadening of the Zener-Landau tunneling fields decreases with temperature for the $|1/2, 1/2\rangle$ to $|1/2, -1/2\rangle$ transitions but are independent of temperature for the $|3/2, 3/2\rangle$ to the $|3/2, 1/2\rangle$ transitions [12]. This behavior is exactly what is expected from a sample containing weak easy-plane spin anisotropy. At sufficiently low temperatures, only the $S = 3/2$ and $S = 1/2$ states are relevant, and the field-dependent crossing of these states depends on whether the magnetic field is parallel or perpendicular to the easy-plane. The broadening is proportional to the difference of the magnetic anisotropy energy for the different spin configurations involved. Due to the small anisotropy in V_{15} the effect will be small. Although it is not possible to translate the DFT obtained anisotropy energies directly to the quantum mechanical many-spin ground state discussed here, we obtain from these energies tunnel field broadenings between 0.1 T to 0.48 T which envelope the experimentally observed field broadening of about 0.2 T [12]. In powdered samples, the small easy-plane anisotropy would lead to a broadening in the tunneling field and in single crystals the effect would change the tunneling fields as a function of field orientations.

To summarize, we have performed accurate all-electron density-functional calculations on the V_{15} cluster as a function of geometry and spin configuration. By dynamically coupling the mean-field density-functional approach to exact-diagonalization of a many-spin Heisenberg representation we have efficiently determined the lowest density-functional configurations and the entire Heisenberg spin excitation spectrum. Our calculations suggest that the small experimentally observed orientational dependence of the tunneling field for the $M_s=3/2$ to $M_s=1/2$ is a signature of configuration dependent magnetic anisotropy in this molecule. The method used here is general and allows one to characterize both sys-

tems which are potentially useful for magnetic storage (Mn_{12} , Fe_8) and systems which show quantum coherence, such as the one studied here.

This work was supported in part by ONR grant N0001498WX20709 and N0001400AF00002. Computations were performed at the DoD Major Shared Resource Centers. We thank I. Chiorescu for enlightening discussions.

† Current address: MPI für Festkörperforschung, Postfach 80065, D-70506 Stuttgart, Germany

- [1] R. F. Service, *Science* **287**, 1902 (2000); S. Sun, C. B. Murray, D. Weller, L. Folks, and A. Moser *Science* **287**, 1989 (2000).
- [2] A. Caneschi, D. Gatteschi, C. Sangregorio, R. Sessoli, L. Sorace, A. Cornia, M. A. Noval, C. Paulsen and W. Wernsdorfer, *J. Magnetism and Magn. Mat.* **200**, 182 (1999) and references there.
- [3] J. Friedman, M. P. Sarachik, J. Tejada, J. Maciejewski and R. Ziolo, *Phys. Rev. Lett.* **76**, 3820 (1996); L. Thomas, F. Lioni, R. Ballou, D. Gatteschi, R. Sessoli and B. Barbara, *Nature (London)* **383**, 145 (1996).
- [4] C. Sangregorio, T. Ohm, C. Paulsen, R. Sessoli and D. Gatteschi, *Phys. Rev. Lett.* **78**, 4645 (1997).
- [5] A. Müller and J. Döring, *Angew. Chem. Int. Ed.* **27**, 1721 (1988).
- [6] D. Gatteschi, L. Pardi, A. L. Barra, A. Müller and J. Döring, *Nature* **354**, 463 (1991).
- [7] N. D. Mermin, *Physics Today*, July, 11 (2000); D. P. DiVincenzo, D. Loss, *J. Magnetism and Magn. Mat.* **200**, 202 (1999).
- [8] A. Müller and J. Döring, *Z. anorg. allg. Chem.* **595**, 251 (1991).
- [9] J. P. Perdew, K. Burke and M. Ernzerhof, *Phys. Rev. Lett.* **77**, 3865 (1996).
- [10] M. R. Pederson and K. A. Jackson, *Phys. Rev. B*, **41**, 7453 (1990); K. A. Jackson and M. R. Pederson, *Phys. Rev. B* **42**, 3276 (1990).
- [11] C. S. Hellberg, W. E. Pickett, L. L. Boyer, H. T. Stokes and M. J. Mehl, *J. Phys. Soc. Jpn.* **68**, 3489 (1999).
- [12] I. Chiorescu, W. Wernsdorfer, A. Müller, H. Bögge and B. Barbara, *Phys. Rev. Lett.* **84**, 3454 (2000); cond-mat/9911180.
- [13] J. B. Goodenough, *Magnetism and the Chemical Bond* (Wiley, New York, 1963).
- [14] V. V. Dobrovitski, M. I. Katsnelson, B. N. Harmon, *Phys. Rev. Lett.* **84**, 3458 (2000).
- [15] D. Gatteschi, L. Pardi, A. L. Barra and A. Müller, *Mol. Engin.* **3**, 157 (1993).
- [16] W. E. Pickett, *Phys. Rev. Lett.* **79**, 1746 (1997)
- [17] I. Chaplygin, R. Hayn and K. Koepnick, *Phys. Rev. B* **60**, R12557 (1999)
- [18] M. R. Pederson and S. N. Khanna, *Phys. Rev. B* **60**, 9566 (1999).
- [19] M. R. Pederson and S. N. Khanna, *Chem. Phys. Lett.* **307**, 253, (1999); M. R. Pederson and S. N. Khanna, *Phys. Rev. B* **59**, R693 (1999).
- [20] A. L. Barra, D. Gatteschi, and R. Sessoli, *Phys. Rev. B* **56**, 8192 (1997).